Article

Strength Performance and Stabilization Mechanism of Fine Sandy Soils Stabilized with Cement and Metakaolin

Shengnian Wang [1,2] , **Xingjin Zhang** [2], **Peng Zhang** [1,2,*] and **Zewei Chen** [2]

1   Jiangsu Province Engineering Research Center of Transportation Infrastructure Security Assurance Technologies, Nanjing Tech University, Nanjing 211816, China
2   College of Transportation Science & Engineering, Nanjing Tech University, Nanjing 211816, China
*   Correspondence: zhangpeng-mail@njtech.edu.cn

Abstract: Enhancing strength performance while reducing cement consumption for soil stabilization is the key to improving the economic benefits of engineering construction projects like retaining structures of underground engineering, subgrade bases, and foundation reinforcement. This study employed metakaolin as the additive to realize these two aims. A series of compression and microstructural observation tests on cement- and metakaolin-stabilized fine sandy soils (CMSFSS) were conducted with different cement–metakaolin ratios, water–binder ratios, dosages of the binder (the mixture of cement and metakaolin), and curing ages. The influences of these factors on the mechanical performance of the CMSFSS were studied. The empirical relationships between compressive strength and these influence factors were discussed. Then, the strengthening mechanism of the CMSFSS at different curing ages was investigated. The results showed that the optimal cement–metakaolin ratio for fine sandy soil stabilization was 5:1, which did not change with the total consumption of cement and metakaolin. The compressive strength of the CMSFSS decreased linearly with the water–binder ratio but increased linearly with the curing age. Four empirical prediction formulas about these strength-influencing factors were summarized. The evolution of microstructural characteristics discovered by scanning electron microscope and mercury intrusion tests showed that the hydrated gels in CMSFSS were being formed during the early curing age and resulted in decreasing pore sizes with an initial rapid rate and then a slower rate over the curing age. The gradual disappearance of calcium hydroxide (by-products of cement hydration) over the curing age proved the promoting effect of metakaolin on the strength improvement of cement-stabilized fine sandy soils. This study can provide a reference for applying cement and metakaolin in soil stabilization practices.

Keywords: soil stabilization; mechanical property; strengthening mechanism; empirical formula; sandy soil; metakaolin

1. Introduction

Economic globalization is continuously driving the accelerated development of urbanization construction, especially in those regions along rivers and coasts [1,2]. However, fine sandy strata are always widely distributed in those areas. Due to their high natural water content, high compressibility, low strength, and the easily broken characteristics of particles, underground space practices would inevitably suffer from engineering problems such as low bearing capacity, high settlement, and poor stability [3–6]. If those sandy strata are not adequately treated, the uneven settlement and shear cracking of ground surfaces would unexpectedly occur and might even lead to severe damage to buildings [7]. Successfully implementing engineering construction on sandy strata is thus always a hot issue in the construction of towns and cities in many countries [8–10]. Cement-stabilized soil is the traditional construction material for underground engineering practices. It possesses the advantages of local extraction, reduced transportation, convenient construction, and low price, and has been widely used in foundation reinforcement, channel impermeability,

deep foundation pits, earth and rock dams, and other projects [11,12]. However, excessive cement dosage in actual soil stabilization practices would result in excessive volume shrinkage due to water evaporation during the hardening process of cement-stabilized soil, causing significant dry shrinkage and cracking defects [13]. Moreover, cement is a high-cost and high energy industrial product. Its production is usually accompanied by massive greenhouse gas emissions, leading to the intensification of the global warming crisis [14]. Therefore, effectively improving the strength performance of cement-stabilized soils and reducing cement consumption is a meaningful way out for the sustainable development of resources and the environment, as well as the promotion of engineering economic benefits.

Additives are an effective way to improve the mechanical performance and durability of cement-stabilized soils. Tuncer et al. [15] studied the strengthening effect of fly ash on cement-stabilized fine-grained soils and proved the contributions of fly ash in improving the bearing capacity of the soil. Kolias et al. [16] found that free CaO in fly ash could react with clay minerals to form calcium aluminosilicate and other hydrates. Soumendra [17] reported that the mixture of fly ash and dolomite could improve the bearing capacity of expansive soils and reduce their liquid and plastic limits, plasticity indices, and swelling indices. Kamei et al. [18] studied the feasibility of waste gypsum and fly ash on the durability of cement-stabilized soils when suffering from freeze–thaw and dry–wet environmental effects, and demonstrated that the incorporation of waste gypsum and fly ash could effectively improve the strength and durability of cement-stabilized soils. Wu et al. [19] indicated that the strength of dredged soils stabilized with cement and steel slag in a seawater erosion environment increased with erosion time, while the opposite was true for the case without adding steel slag. Choobbasti et al. [20] investigated the effects of nano-silica on the microstructure and strength of cement-stabilized sandy soil and found that the incorporation of a certain amount of nano-silica could enhance the strength of sandy soil. All of these studies suggested that a powdered precursor with a high content of silicon and aluminum minerals could promote the performance improvement of soils.

Metakaolin is a thermally activated aluminosilicate material with high pozzolanic activity. The anhydrous aluminum silicate active ingredient can react with the calcium hydroxide produced by the hydration of cement to generate hydrated calcium aluminum feldspars and CSH gels [21,22]. They also can polymerize aluminosilicate network structures with ionic and covalent bonds as the primary bonds and van der Waals bonds as the supplement bonds in the geopolymer under the induction of activators and hardeners such as strong alkaline or sulfate [23]. Hence, metakaolin should be available to improve the engineering performances of soils. Kolovos et al. [24] found that adding metakaolin could reduce the shrinkage of cement-stabilized clay and improve its microstructural compactness. Wu et al. [25] and Wang et al. [26] reported that metakaolin could improve the compressive and splitting strength of cemented soils and lead to more hydration products and denser microporous distribution. Deng et al. [27] pointed out that metakaolin could be used to replace cement partly for soft marine clay stabilization. Zhang [28] and Ma [29] pointed out that the strength of cement-stabilized soils initially increased and then decreased with the increasing dosage of metakaolin. Xing et al. [30] further indicated that there was a limit value for the amount of metakaolin in soil stabilization with cement. Wu et al. [31] demonstrated that the contribution of metakaolin to the performance improvement of cement-stabilized soils was more significant than that of steel slag. Tan et al. [32] found that metakaolin could effectively improve the long-term strength of silty soils stabilized with cement and lime. These studies evidently could provide a vital reference for the research and application of soft soil stabilization. However, sandy soils mainly consist of sand and silt particles with few clay particles. How could metakaolin improve the engineering performance of sandy soils? What is the maximum amount of cement that can be saved by metakaolin? The current research obviously cannot ensure the same effects with the same technical parameters. A more in-depth study is thus needed.

Given these considerations, this study similarly employed metakaolin as the additive to partially replace cement for fine sandy soil stabilization since it could play a significant role in the hydration reaction of cement or undergo covalent polymerization due to the alkaline environment formed by calcium hydroxide. Both of these two chemical reactions could produce gels to fill the pores in fine sandy soils, improving their structural compactness and strength. To investigate the contribution of metakaolin on the mechanical performance improvement of cement-stabilized fine sandy soils, a series of indoor compression tests were conducted. The influences of the cement–metakaolin ratio, the water–binder ratio, the dosage of the binder (the mixture of cement and metakaolin), and the curing age on the strength performance of fine sandy soils were explored. The empirical strength prediction formulas about these influencing factors were summarized. Microstructure observation tests, including Scanning Electronic Microscopy (SEM) and Mercury Intrusion Porosimetry (MIP) tests, were carried out to explain the stabilization mechanism of the cement- and metakaolin-stabilized fine sandy soils (CMSFSS).

2. Materials and Methods

2.1. Materials and Apparatus

2.1.1. Materials

Sandy soil. The testing soil was collected from a construction site at the Yangtze River floodplain area of Pukou District, Nanjing, China. As shown in Figure 1, the texture of this soil is mainly fine gray-brown sand with a few silty particles. The in situ survey results show that this soil was located at −17.93 m above sea level. The natural unit weight of this soil was 19.4 kN/m^3. The natural water moisture content was 24.1%. The initial pore ratio was 0.678. The shear strength, including cohesion and internal friction angle, were 4.3 kP and 29.3°, respectively. Considering that the sizes of some sand particles were larger than 2 mm, the natural sandy soils used in this study were dried and passed through a 2 mm sieve to ensure the homogeneity of specimens.
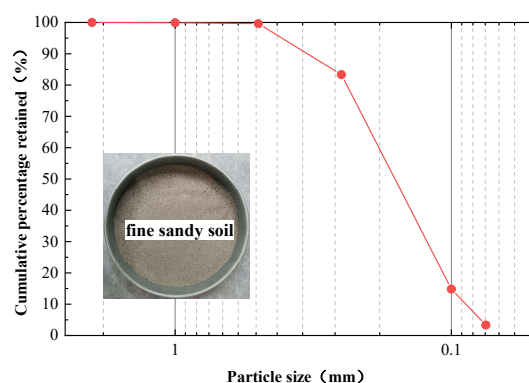

Figure 1. Grading curve of fine sandy silt used in this study.

Cement. The cement used in this study was produced by Jiangxi Xinyu Fenyi Conch Cement Co., Ltd., Xinyu, China. It was P.O. 42.5 ordinary Portland cement.

Metakaolin. The metakaolin was a 1250 mesh white powder produced by Henan Bairun Casting Materials Co., Ltd., Gongyi, China. As shown in Figure 2, it contains more than 94% silicon and aluminum minerals. The specific chemical components and proportions are listed in Table 1.

Figure 2. Sample of powdered metakaolin.

Table 1. Primary chemical components of metakaolin.

Chemical Component	Al$_2$O$_3$	SiO$_2$	Fe$_2$O$_3$	TiO$_2$
Proportion (%)	41.30	53.03	0.81	1.00

2.1.2. Apparatus

A microcomputer-controlled electronic universal testing machine was used for mechanical property testing, which could realize four kinds of closed-loop controls by an AC servo driver and motor, including loading force, sample deformation, crossbeam displacement, and testing process. The designed maximum loading force of this machine was 20 kN. The loading rate was 0.001–500 mm/min with a control accuracy of ±1% (0.001~10 mm/min). The deformation measurement accuracy was ±0.5%. The control ranges of constant force, strain, and displacement were 0.2–100% *FS* (*FS* is full scale). To ensure the reliability and stability of testing results that might be affected by the size of specimens, the loading rate of unconfined compression tests was 1.0 mm/min. For microstructural observation, a JSM-6510 electron microscope scanner was used to observe the surface structural characteristics of samples by secondary electrons, backscattered electrons, and characteristic X-rays. The acceleration voltage range of this device was 0.3–30 kv. The magnification ranged from 18–300,000 times with a resolution of 3 nm. The SEM images of the CMSFSS at two magnifications were also collected at an acceleration voltage range of 15 kv. A GT-60 automatic mercury porosimeter was used to measure the samples' macro- and micropore distribution. This porosimeter had two low-pressure stations and two high-pressure stations. The former was used to fill mercury and roughly measure the diameter of the pores, and the latter could measure pore volume in diameters from 0.0036 μm to 950 μm. The mercury pressure range of the low-pressure stations could vary from 1.5 kPa to 350 kPa. The mercury pressure range of the high-pressure stations could vary from 140 kPa to 420 MPa. When testing, the surface tension of mercury was set to 0.48 N/m, the contact angle was set to 140°, and the maximum pressure was set to 345 MPa.

2.2. Experimental Scheme

This study aimed to explore the influence of the cement–metakaolin ratio, the water–binder ratio, the dosage of the binder, and the curing age on the strength performance of sandy soils and explain their stabilization mechanism. Therefore, the single-variable method was used in the experimental design of this study.

(1)　Tests for the cement–metakaolin ratio

A higher dosage of metakaolin did not mean a better performance improvement for cement-stabilized soils. Wang et al. [26] suggested that the mixing ratio of cement and coal–metakaolin should be 6.5:1–4.0:1. Therefore, this study selected the cement–metakaolin ratios of 3:1, 4:1, 5:1, 6:1, and 7:1 to explore the influence of the cement–metakaolin ratio on

the compressive strength evolution of the CMSFSS to determine the optimal ratio for sandy soil stabilization. Since the optimal cement–metakaolin ratio was the primary condition for the other tests, a constant total dosage of cement and metakaolin and water–binder ratio were adopted. Here the dosages of the binder were designed as 10%, 15%, 20%, and 25%. The water–binder ratio was 0.6. This ratio was an assumed value determined by trial and error, based on the sensual fluidity of the soil mass.

(2) Tests for the water–binder ratio

It is well known that the mechanical performance of cement-stabilized soils would be weakened with an increase in the water–binder ratio since too much free water could cause more pores to be left in the soil after stabilization. Of course, the value of the water–binder ratio should not be too small due to difficulties in engineering construction practices. For a comprehensive view of the scheme, the water–binder ratio was designed as 0.4, 0.6, 0.8, 1.0, and 1.2. The cement–metakaolin ratio was the optimal value obtained from the above tests. The dosage of the binder was 15% since this value was commonly used in engineering practices.

(3) Tests for the dosage of the binder

Generally, the mechanical performance improvement of problematic soils will be enhanced with an increase in binder dosage. The higher the binder dosage, the better the mechanical performance improvement of the soil was. However, many studies similarly indicated that the mechanical performance increment of soil would decrease rapidly when the binder dosage reached a certain level. Therefore, the dosages of the binder were designed as 10%, 15%, 20%, 25%, and 30% to investigate their influence on the mechanical performance of sandy soils. The cement–metakaolin ratio was the optimal value obtained from the tests for the cement–metakaolin ratio. The water–binder ratio was the recommended value obtained from the above tests for the water–binder ratio.

(4) Tests for the curing age

The compression tests on the CMSFSS cured for 3, 7, and 28 days were carried out to explore their strength evolution. Here, the cement–metakaolin ratio was the optimal value obtained from the tests for the cement–metakaolin ratio. The water–binder ratio was the recommended value obtained from the tests for the water–binder ratio. The dosage of the binder was 15%.

(5) Scanning Electronic Microscopy (SEM) tests

The microstructural images by SEM at magnifications of 1000 and 5000 times were collected after the CMSFSS were cured for 3, 7, and 28 days. Then, their structural evolution and material composition over curing time were tracked and discussed. Here the cement–metakaolin ratio was the optimal value obtained from the tests for the cement–metakaolin ratio. The water–binder ratio was the recommended value obtained from the tests for the water–binder ratio. The dosage of the binder was 15%. Of course, it should be noted that the results of microstructural observation on the CMSFSS may not be representative of the full-scale characteristics of the whole sample in some cases due to their small observation range.

(6) Mercury Intrusion Porosimetry (MIP) tests

MIP tests on the CMSFSS after being cured for 3, 7, and 28 days were similarly conducted to observe their internal pore characteristic evolution including their distribution, size, and connectivity. The cement–metakaolin ratio, the water–binder ratio, and the dosage of the binder were the same as in the SEM tests.

For brevity and readability on the experimental scheme design, the parameters for each experimental scheme are listed in Table 2.

Table 2. The designed experimental parameters for each scheme.

Testing Schemes	Designed Parameters			
	Cement–Metakaolin Ratio	Water–Binder Ratio	Dosage of the Binder (%)	Curing Age (d)
Tests for the cement–metakaolin ratio	3:1, 4:1, 5:1, 6:1, 7:1	0.6	10%, 15%, 20%, 25%, 30%	7
Tests for the water–binder ratio	5:1	0.4, 0.6, 0.8, 1.0, 1.2	15	7
Tests for the dosage of the binder	5:1	0.6	10%, 15%, 20%, 25%, 30%	7
Tests for the curing age	5:1	0.6	15	3, 7, 28
SEM tests	5:1	0.6	15	3, 7, 28
MIP tests	5:1	0.6	15	3, 7, 28

2.3. Specimen Preparation

It is worth noting that all mass mixing ratios in this study were based on the dry weight of the soil. As shown in Figure 3, when sampling, the dry fine sandy soils, cement, and metakaolin were weighed following the designed experimental scheme and blended thoroughly first. Then, the water was added into these mixtures and mixed until the sample was uniformly mixed. The mixing time was controlled for 10–20 min at least according to practical experience. When the mixture was ready, it was poured into a cylindrical mold with a diameter of 50 mm and a height of 100 mm. Each specimen in the mold would be tamped vertically 15 times from the edge to the center by a ramming bar in the spiral direction. A scraper was inserted and extracted several times along the mold's inner surface to eliminate air and ensure the integrity of the specimen's surface. When these steps were completed, the final prepared specimens were placed in a standard curing environment for 24 h and then de-molded and cured at the same conditions until the target curing age was reached. According to the Standard for Geotechnical Testing Method GB/T 50123-2019 issued by the Ministry of Housing and Urban–Rural Development of China, the temperature and humidity of a standard curing environment is $20 \pm 3\ °C$ and 90–95%, respectively. Since significant differences in the weight of specimens could appear after removing the mold, six specimens were prepared in the initial specimen preparation. Only three with the minimum weight error were selected for the final tests to ensure the experimental data's high reliability.

(**a**) Dry mixture   (**b**) Wet sample   (**c**) Cylindrical specimens

Figure 3. Specimen preparation.

For microstructural observation, the cured specimens were cut into small pieces with sizes of 5 mm × 5 mm × 5 mm and 10 mm × 10 mm × 10 mm. Then, they were polished and carefully leveled for SEM image collection and the Mercury Intrusion test. The small specimens for SEM tests were sprayed with a gold layer and vacuumed to prevent the high-energy electron beam from being absorbed or scattered on the air molecules during the testing process.

3. Results and Analysis

3.1. Cement–Metakaolin Ratio

Figure 4 illustrates the unconfined compressive strength of the CMSFSS with different cement–metakaolin ratios, in which the cement–metakaolin ratios were 3:1, 4:1, 5:1, 6:1, and 7:1, the dosages of the binder were 15%, 20%, 25%, and 30%, the water–binder ratio was 0.6, and the curing age was seven days. It could be observed that the unconfined compressive strength of the CMSFSS with dosages of cement and metakaolin of 10%, 15%, 20%, and 25% initially increased and then decreased with increasing cement–metakaolin ratio. The maximum compressive strength of fine sandy soils with the same dosage of the binder was always obtained when the cement–metakaolin ratio was 5:1. Namely, the cement–metakaolin ratio did not change with the total dosage of cement and metakaolin. Further, the unconfined compressive strength of the CMSFSS would not be affected by the dosage of the binder when their mixing ratio was 5:1. The main reason for this outcome may be that when the cement–metakaolin ratio was greater than 5:1, the calcium hydroxide formed by the hydration of cement could fully rehydrate with the silicon aluminum oxides in metakaolin or covalently polymerize the silicon aluminum oxides in metakaolin in an alkaline environment, and more cementitious materials were formed to fill the pores in the fine sandy soils, thereby effectively improving the impermeability of the fine sandy soil. When the cement–metakaolin ratio was less than 5:1, the dosage of metakaolin was relatively high. Namely, the dosage of cement was reduced relatively. The calcium hydroxide formed by the hydration of cement could not fully react with the silicon–aluminum minerals in the metakaolin to form CSH gels or covalently polymerize the silicon–aluminum minerals to form geopolymers. Hence, the compressive strength of the CMSFSS decreased.
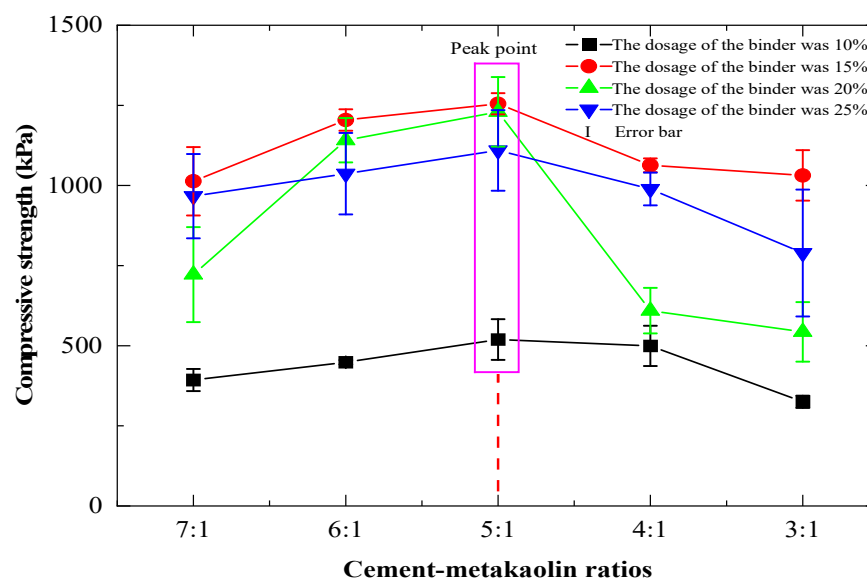

Figure 4. Compressive strength of fine sandy soils with different cement–metakaolin ratios.

3.2. Water–Binder Ratio

Figure 5 presents the unconfined compressive strength of the CMSFSS with different water–binder ratios, in which the water–binder ratios were 0.4, 0.6, 0.8, 1.0, and 1.2, the cement–metakaolin ratio was 5:1, the dosage of the binder was 15%, and the curing age was seven days. The unconfined compressive strength of the CMSFSS decreased nonlinearly with the water–binder ratio. The greater the water–binder ratio was, the more significant the decrease was [4]. One reason for this change may be that a high water–binder ratio would significantly increase the amount of residual pores after hardening in the CMSFSS due to high amounts of free water evaporation. Other reasons may be that the specific surface area of the metakaolin was relatively small or the excessive water may be detrimental

to the silicon–aluminum minerals in the metakaolin reacting with calcium hydroxide. Therefore, their strength performance decreased with the water–binder ratio. Considering the workability of the CMSFSS and the aim to enhance their compressive strength as much as possible, a water–binder ratio of 0.6 was used for the subsequent tests in this study.
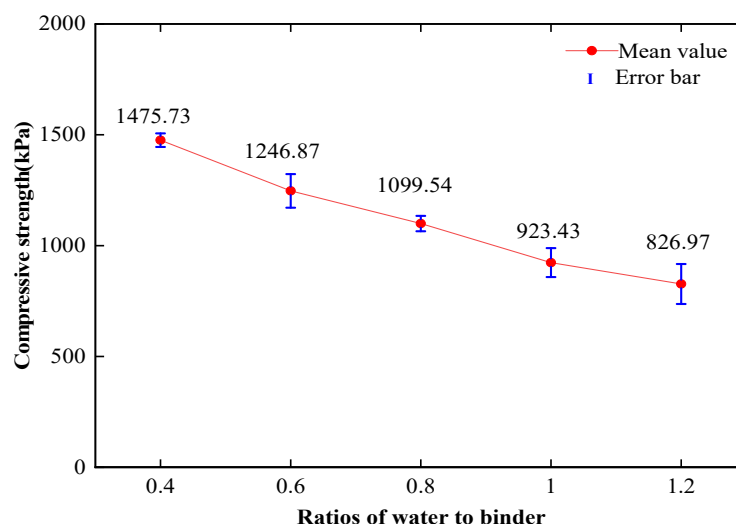

Figure 5. Compressive strength of CMSFSS with different ratios of water to binder.

3.3. Dosage of Binder

Figure 6 shows the compressive strength of CMSFSS with different dosages of the binder, in which the dosages of the binder were 15%, 20%, 25%, and 30%, the cement–metakaolin ratio was 5:1, the water–binder ratio was 0.6, and the curing age was seven days. When the dosage of the binder increased from 10% to 25%, the compressive strength of the CMSFSS increased linearly with the dosage of the binder, and there was a good correlation between compressive strength and the dosage of the binder. This conclusion was consistent with the research conclusion on cement soil [33]. However, when the dosage of the binder was higher than 25%, the compressive strength increments of the CMSFSS decreased. This improvement rate reduction implied that more binder consumption did not always contribute positively to the strength performance improvement of the soil when the dosage of the binder reached a certain level. Moreover, a high binder consumption was evidently uneconomical. Hence, the dosage of the binder for soil stabilization should be limited to below 25%.
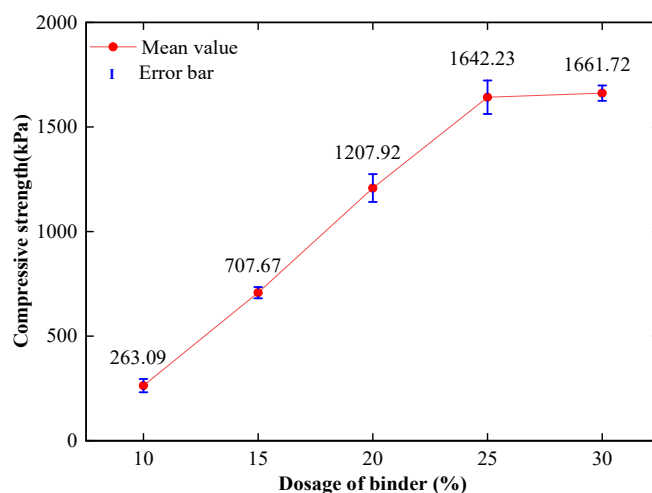

Figure 6. Compressive strength of fine sandy soils with different dosages of the binder.

3.4. Curing Age

Figure 7 shows the compressive strength of CMSFSS under different curing ages, in which the curing ages were 3, 7, and 28 days, the cement–metakaolin ratio was 5:1, the water–binder ratio was 0.6, and the dosage of the binder was 15%. The compressive strength of the CMSFSS increased with the curing age [34]. The compressive strength of the CMSFSS after being cured for 28 days was roughly two times and five times that for seven days and three days. The compressive strength of the CMSFSS after being cured for seven days was about three times that for three days. These differences indicated that the strength performance improvement rate of the CMSFSS decreased with the curing age. The main reason for this change may be that the primary component of the gel material was cement, which was the dominant controlling factor for the strength performance improvement of the CMSFSS. Meanwhile, the alkaline environment produced by cement hydration could activate the silicon–aluminum minerals in the metakaolin to react with the calcium hydroxide or covalently polymerize into geopolymer gels over the curing age. Therefore, their strength performance improvement was similar to pure cement stabilization.
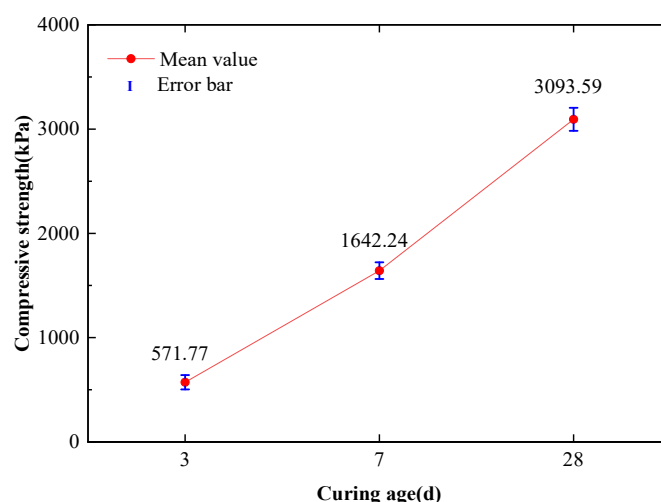

Figure 7. Compressive strength of CMSFSS after different curing times.

4. Discussion

Since the mechanical performance improvement of fine sandy soils was significantly affected by the dosage of the binder, the water–binder ratio, and the curing age, the relationships between compressive strength and these influence factors are further discussed below.

4.1. Relationship of Compressive Strength vs. Water–Binder Ratio

Many studies have addressed the quantitative relationship between the compressive strength of cement soil and the water–binder ratio. Therefore, to further building the compressive strength prediction formula for CMSFSS about the water–binder ratio could provide a good reference for their engineering design and application. Suk et al. [35] proposed an exponential prediction formula for the strength of cement soil with the water–binder ratio as a variable, which could be improved and rewritten as:

$$q_c = a(w/c)^{-b} \tag{1}$$

where q_c is the unconfined compressive strength, w/c is the water–binder ratio, and a and b are fitting parameters.

Figure 8a presents the fitting curve of the experimental data with the above empirical formula. There was an excellent correlation between the compressive strength of the CMSFSS and their water–cement ratio. The fitting parameters a and b were 1.0×10^3

and 0.5, respectively, with a high correlation coefficient of 0.976. To further demonstrate its applicability to different fine-grained soils, this study employed the testing results on cement-stabilized clay and silty clay to fit this formula [36,37]. As shown in Figure 8b, the measured and predicted values of these soils were all close to the bisecting line, which indicated that the proposed empirical formula could accurately describe the relationship between the compressive strength and water–cement ratio for inorganic binder stabilized soils. Namely, the fitting parameters *a* and *b* could be 1.0×10^3 and 0.5, respectively.
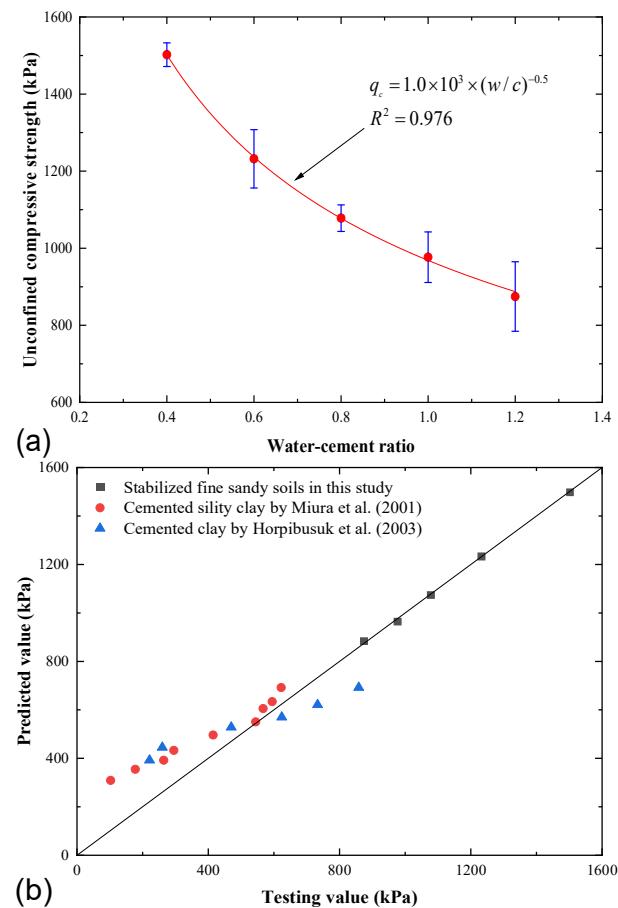

Figure 8. Data fitting and verification. (**a**) Fitting curve between compressive strength and the ratio of water to binder; (**b**) Comparison of predicted and testing values [36,37].

4.2. Relationship of Compressive Strength vs. Dosage of Binder

Since the compressive strength of the CMSFSS had an ideal linear development with the dosage of the binder when it was less than 25%, a linear fit was applied to describe this relationship. When the dosage of the binder was higher than 25%, the compressive strength improvement of the CMSFSS was limited. Their compressive strength could be approximately regarded as constant. Hence, the relationship between the compressive strength and the dosage of the binder could be expressed by a piecewise function as:

$$q_c = \begin{cases} \lambda(p_{cm} - 0.1) + q_{c10}, \ 0 \leq p_{cm} \leq 25\% \\ q_{cu}, \ 25\% \leq p_{cm} \leq 30\% \end{cases} \tag{2}$$

where p_{cm} is the dosage of the binder (%), λ is a fitting parameter related to the properties of the binder itself, q_{c10} is the unconfined compressive strength of the soil stabilized with 10% binder, and q_{cu} is the meaning unconfined compressive strength of the stabilized soil with the dosage of the binder greater than 25%.

Figure 9a presents the fitting curve of the experimental data with the above empirical formula. A good correlation could be found between the compressive strength of the CMSFSS and the dosage of the binder. The linear fit achieved a high correlation coefficient of 0.998, and the fitting parameters λ and q_{s10} were 9.275×10^3 and 263, respectively. Similarly, the testing results of the cement-stabilized clay, silty clay, and silty soil in some studies were employed to fit this formula to verify its applicability to different fine-grained soils [38–40]. As shown in Figure 9b, these soils' measured and predicted values were all close to the bisecting line. This indicates that the proposed empirical formula could describe the relationship between the compressive strength and the dosage of the binder for different stabilized soils.
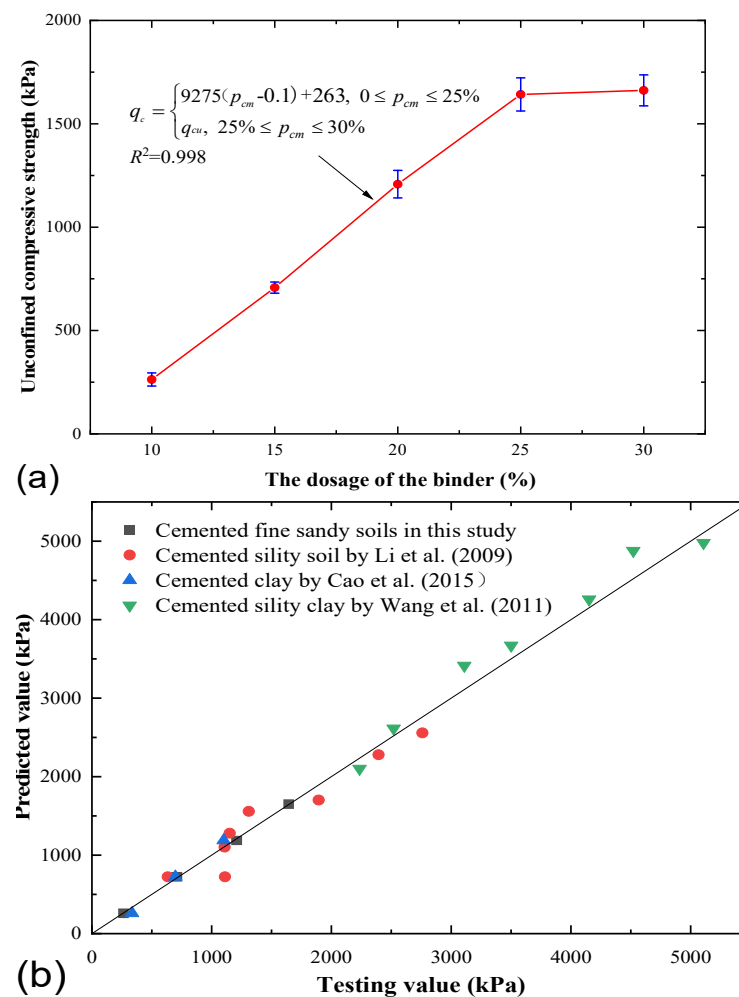

$$q_c = \begin{cases} 9275(p_{cm}-0.1)+263, & 0 \leq p_{cm} \leq 25\% \\ q_{cu}, & 25\% \leq p_{cm} \leq 30\% \end{cases}$$

$R^2 = 0.998$

(a)

- ■ Cemented fine sandy soils in this study
- ● Cemented sility soil by Li et al. (2009)
- ▲ Cemented clay by Cao et al. (2015)
- ▼ Cemented sility clay by Wang et al. (2011)

(b)

Figure 9. Data fitting and verification. (**a**) Fitting curve between compressive strength and the dosage of binder; (**b**) Comparison of predicted and testing values [38–40].

4.3. Relationship of Compressive Strength vs. Dosage of Binder and Water–Binder Ratio

The compressive strength of the CMSFSS was not only controlled by the dosage of cement and metakaolin but was also affected by the water–binder ratio. Therefore, an improved empirical prediction formula based on the Equations (1) and (2) was proposed by using the dosage of binder as the internal link. Namely,

$$q_c = (\alpha p_{cm}+\mathrm{k})/(w/c)^{\eta} \tag{3}$$

where α, *k*, and η are fitting parameters.

Figure 10 illustrates the variations in the compressive strength of CMSFSS with different dosages of binder and water–cement ratios. The compressive strength of the CMSFSS

correlated well with the water–cement ratio and the dosage of the binder. A lower dosage of the binder and higher water–binder ratio would result in a poor strength performance improvement of the CMSFSS. The steepness of the fitting curve at the low water–binder ratio was more significant than that at the high water–binder ratio, indicating that the contribution of the water–binder ratio might be more remarkable than the dosage of the binder.
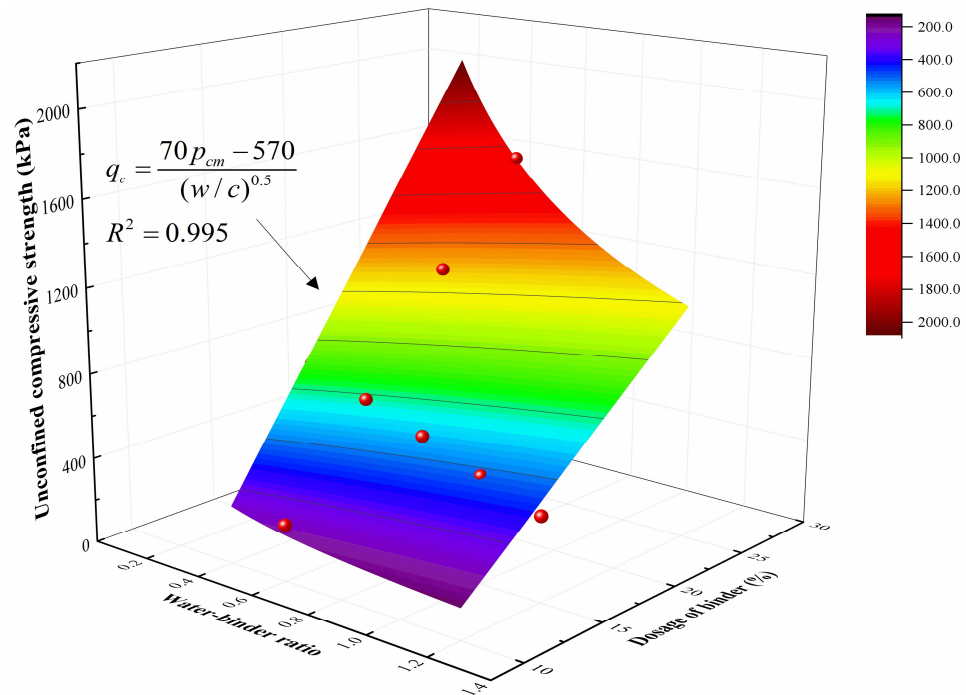

$$q_c = \frac{70\,p_{cm} - 570}{(w/c)^{0.5}}$$

$$R^2 = 0.995$$

Figure 10. Relationship among compressive strength, the dosage of binder, and water–binder ratio.

4.4. Relationship of Compressive Strength vs. the Curing Age

According to the empirical formula proposed by Suksun et al. [41] and the law reflected by the results shown in Figure 7, an empirical prediction formula for the compressive strength of the CMSFSS in terms of the curing age was proposed as:

$$q_c = q_{c28}[m + n \log_{10}(T + 1)], T \geq 0 \tag{4}$$

where *m* and *n* are fitting parameters, and *T* is the curing age.

Figure 11a shows the fitting curve of the experimental data with the above empirical formula. This formula described the compressive strength improvement of the CMSFSS with the curing age well. Similarly, to verify its applicability to other fine-grained soils, the testing results on cement-stabilized clay, and silty and soft marine soils in some studies were collected and fitted following the proposed empirical prediction formula [25,41,42]. The outcomes in Figure 11b showed that these soils' measured and predicted values were all close to the bisecting line. Namely, the proposed formula could be used to predict the strength performance of inorganic binder stabilized soils at a specific curing age.
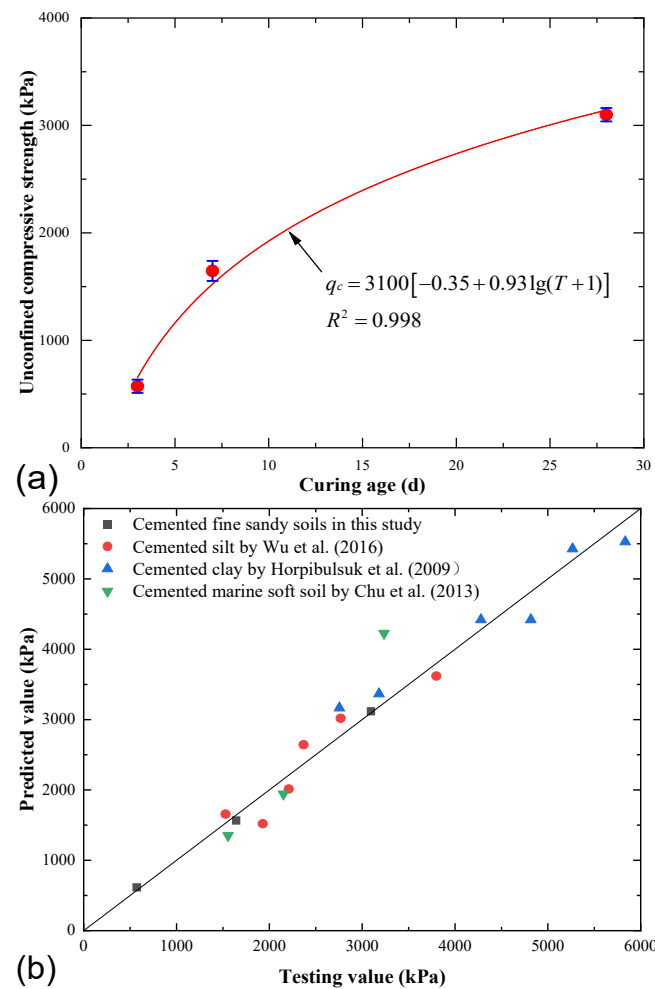
In figure (a):
$$q_c = 3100\left[-0.35 + 0.93\lg(T+1)\right]$$
$$R^2 = 0.998$$

Figure 11. Data fitting and verification. (**a**) Fitting curve between compressive strength and curing age; (**b**) Comparison of predicted and testing values [25,41,42].

5. Stabilization Mechanism Analysis

The structural compactness of fine sandy soils determines their mechanical performance to some extent. The metakaolin with high pozzolanic activity could participate in the hydration reaction of cement in an alkaline environment or undergo covalent polymerization due to the alkaline environment formed by calcium hydroxide. Both of these two chemical reactions could produce gels to fill the pores in fine sandy soils, improving the structural compactness of fine sandy soils and thereby enhancing their strength. Therefore, the stabilization mechanism analysis of the CMSFSS was investigated and discussed through microstructural characteristics and intermediate products observed by SEM and MIP, such as the formation of gels and by-products, pore size, pore distribution, and pore connectivity.

5.1. SEM

Figure 12 presents the microstructural images of the CMSFSS at different curing ages. The microstructural characteristics at an early curing age showed that there were a large number of pores with a size greater than 10 μm distributed in the CMSFSS, and a large amount of tiny acicular calcium silicate gels and hexagonal plates of calcium hydroxide were continuously forming on the surface of the soil particles. With the increase in curing age, these acicular calcium silicate gels continued to expand and extend towards the pores between soil skeletons. The size of the internal pores in the CMSFSS continued to decrease. The cluster effect of soil particles became more and more significant. At the same time,

the calcium hydroxide gradually disappeared. It is well known that residual calcium hydroxide, as the by-product of cement hydration, generally would continually increase with the development of the cement hydration process. Our results were just the opposite. The only explanation for this change should be that the metakaolin with high pozzolanic activity participated in the hydration reaction of the cement in an alkaline environment or underwent covalent polymerization due to the alkaline environment due to the calcium hydroxide. When the curing age reached 28 days, most large pores in the CMSFSS had disappeared with the increased rod-shaped and flocculent cementitious substances, and only some tiny pores remained. The significant improvement of the structural compactness and integrity of the fine sandy soil could thus explain why the strength performance of the fine sandy soils was enhanced [43,44].
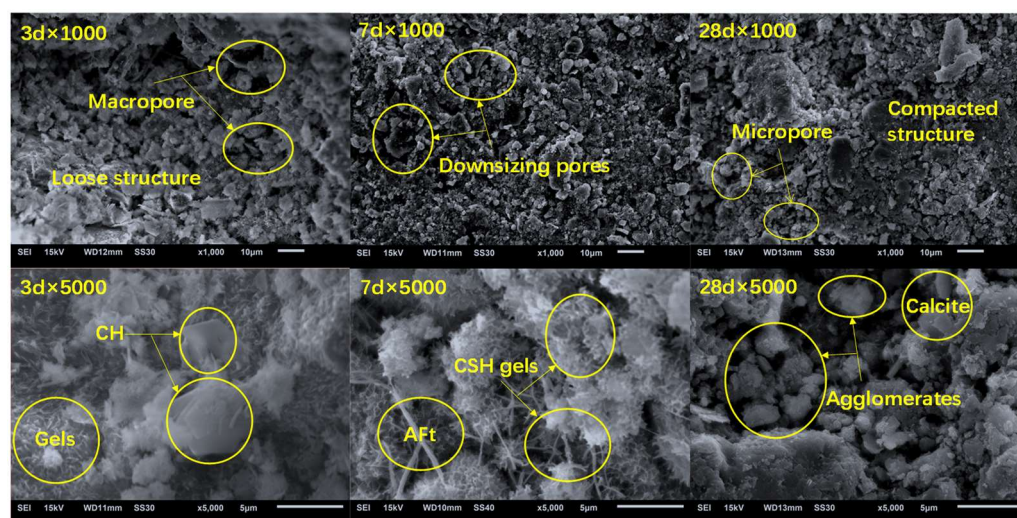
Figure 12. Microstructure evolution of CMSFSS at different curing ages.

5.2. MIP

Figure 13 shows the internal pore characteristics of the CMSFSS at different curing ages. As shown in Figure 13a, the internal pores of the CMSFSS were primarily distributed with a size of less than 5 μm. With the increase in curing age, the mercury intrusion volume in pores of different sizes in the CMSFSS decreased synchronously, especially for pores with sizes of 0.1–10 μm, which had the most typical synchronous shrinkage trend. Figure 13b illustrates the logarithmic differential relationship between pore volume and pore diameter of the CMSFSS at different curing ages. With the increase in curing age, the peak value of the curves gradually decreased and constantly shifted toward smaller pore sizes. The dominant pore size corresponding to the peak value of the curves continued to decrease, implying the shrinkage of internal pores in the CMSFSS. The variations of the peak values and pore sizes for the curing age of 3–7 days were more remarkable than those at 7–28 days, indicating that the filling efficiency of pores by gels in the early curing stages was higher than in the later stages. Namely, the addition of metakaolin promoted the early hydration process of the cementitious material. This finding was consistent with the results given by the SEM tests. Figs. 13 c and d demonstrate the changes in internal porosity and pore connectivity of the CMSFSS with different curing ages. The microstructure porosity and pore connectivity of the samples continued to decrease with the curing age overall. However, their variations at a curing age of 3–7 days were more significant than those at 7–28 days. This difference implied that the physical and mechanical improvement of the CMSFSS might be more likely to occur in the early and middle curing stages.
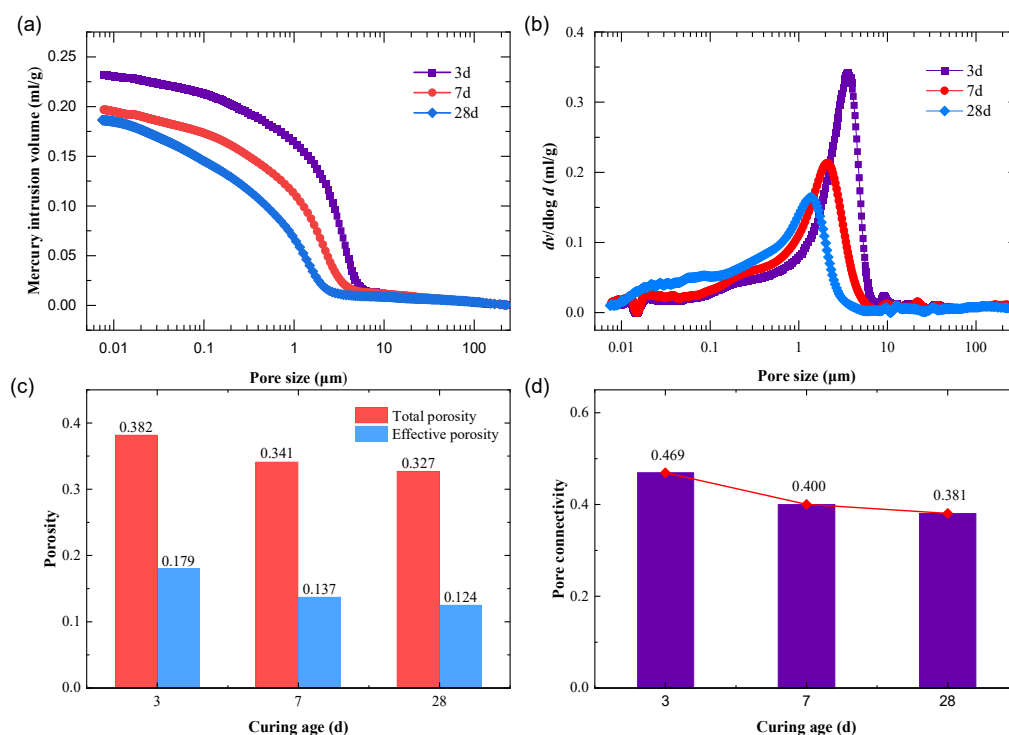
Figure 13. Pore characteristics of CMSFSS at different curing ages. (**a**) Intrusion volume; (**b**) dv/dlog d; (**c**) Porosity; (**d**) Pore connectivity.

6. Conclusions

This study employed metakaolin as the additive to improve the strength performance and reduce cement consumption in fine-grained soil stabilization practices. A series of compression tests investigated the influence of some dominant factors on the strength performance improvement of CMSFSS. Their microstructural stabilization mechanism was explored and discussed through SEM and MIP tests. Some main conclusions were obtained as follows:

(1) The compressive strength of CMSFSS initially increased and then decreased with the cement–metakaolin ratio. Their peak strength value was obtained when the cement–metakaolin ratio was 5:1, and this mixing ratio did not vary with changes in the dosage of cement and metakaolin.

(2) The compressive strength of CMSFSS decreased with the water–binder ratio but increased linearly with the dosage of cement and metakaolin. With the increase curing age, their strength performance improvement was initially fast and then slow. Namely, the contribution of the binder to the strength performance improvement would be very small when the dosage of the binder reached a certain level.

(3) Four empirical formulas regarding the water–binder ratio, the dosage of binder, and the curing age were proposed. Their correctness and applicability were verified by comparing to previous similar studies on fine-grained soils.

(4) The microstructural observations showed that the addition of metakaolin was conducive to producing more cementitious substances to fill the internal pores of the soil, promoting the continuous reduction of pore sizes and thereby improving the structural compactness and integrity of fine sandy soils. The results of this study could provide a reference for soil stabilization practices with cement and metakaolin.

Author Contributions: Conceptualization and writing—review and editing, P.Z.; funding acquisition, data curation, and writing—review and editing, S.W.; investigation, formal analysis, and writing—original draft preparation, X.Z.; investigation and formal analysis, Z.C. All authors have read and agreed to the published version of the manuscript.

References

1. Liu, Y.; He, Q.L.; Jiang, Y.; Sun, M.M.; Chen, E.J.; Lee, F.H. Effect of in Situ Water Content Variation on the Spatial Variation of Strength of Deep Cement-mixed Clay. *Géotechnique* **2018**, *69*, 391–405. [CrossRef]
2. Emmanuel, M.; Hussein, M.; Laurent, L.; Robert, M.E. Physicochemical and Consolidation Properties of Compacted Lateritic Soil Treated with Cement. *Soils Found* **2017**, *57*, 60–79.
3. Pu, S.Y.; Zhu, Z.D.; Zhao, L.M.; Song, W.L.; Wan, Y.; Huo, W.W.; Wang, H.R.; Yao, K.; Hu, L.L. Microstructural Properties and Compressive Strength of Lime or/and Cement Solidified Silt: A Multi-scale Study. *Bull. Eng. Geol. Environ.* **2020**, *79*, 5141–5159. [CrossRef]
4. Zhang, R.; Santoso, A.M.; Tan, T.; Phoon, K.K. Strength of High Water-Content Marine Clay Stabilized by Low Amount of Cement. *J. Geotech. Geoenvironmental Eng.* **2013**, *139*, 2170–2181. [CrossRef]
5. Wang, X.; Cui, J.; Shen, J.H.; Wang, X.Z.; Zhu, C.Q. Particle breakage behavior of a foundation filling material on island-reefs in the South China Sea under impact loading. *Bull. Eng. Geol. Environ.* **2022**, *81*, 1–24. [CrossRef]
6. Wang, X.; Wang, Y.; Liao, C.; Cui, J.; Shen, J.H.; Wang, X.Z.; Zhu, C.Q. Particle breakage mechanism and particle shape evolution of calcareous sand under impact loading. *B Eng. Geol. Environ.* **2022**, *81*, 372. [CrossRef]
7. Dermatas, D.; Dutko, P.; Balorda-Barone, J.; Deok-hyun, M. Evaluation of Engineering Properties of Cement Treated Hudson River Dredged Sediments for Reuse as Fill Material. *J. Mar. Environ. Eng.* **2003**, *7*, 101–124.
8. Liu, Y.; Lee, F.H.; Quek, S.T.; Chen, E.J.; Yi, J.T. Effect of Spatial Variation of Strength and Modulus on the Lateral Compression Response of Cement-admixed Clay Slab. *Géotechnique* **2015**, *65*, 851–865. [CrossRef]
9. Chen, M.; Shen, S.L.; Arulrajah, A.; Wu, H.N.; Hou, D.W.; Xu, Y.S. Laboratory Evaluation on the Effectiveness of Polypropylene Fibers on the Strength of Fiber-reinforced and Cement-stabilized Shanghai Soft Clay. *Geotext. Geomembr.* **2015**, *43*, 515–523. [CrossRef]
10. Li, N.; Zhu, Y.L.; Zhang, F.; Lim, S.M.; Wu, W.Y.; Wang, W. Unconfined Compressive Properties of Fiber-stabilized Coastal Cement Clay Subjected to Freeze—Thaw Cycles. *J. Mar. Sci. Eng.* **2021**, *9*, 143. [CrossRef]
11. Zhang, D.W.; Chen, L.; Liu, S.Y. Key Parameters Controlling Electrical Resistivity and Strength of Cement Treated Soils. *J. Central South Univ.* **2012**, *19*, 2991–2998. [CrossRef]
12. Chen, S.L.; Hou, R.; Ni, C.L.; Wang, J.X. Research on the Mechanical Properties of Cemented Soil Based on Triaxial Compression Tests. *Bull. Chin. Ceram. Soc.* **2018**, *37*, 4012–4017.
13. Thanakorn, C.; Krisdha, T.; Suched, L. Swell-shrink Behaviour of Cement with Fly Ash-stabilised Lakebed Sediment. *Bull. Eng. Geol. Environ.* **2021**, *80*, 2617–2628.
14. Ma, Z.C.; Wang, L. Technical Progess of Emssion-reduction and Utilization of Corbon Dioxide in Cement Industey. *Mater. Rev.* **2011**, *25*, 150–154.
15. Edil, T.B.; Acosta, H.A.; Benson, C.H. Stabilizing soft fine-grained soils with fly ash. *J. Mater. Civ. Eng.* **2006**, *18*, 283–294. [CrossRef]
16. Kolias, S.; Kasselouri-Rigopoulou, V.; Karahalios, A. Stabilisation of cCayey soils with High Calcium Fly Ash and Cement. *Cem. Concr. Compos.* **2004**, *27*, 301–313. [CrossRef]
17. Soumendra, K.M.; Pradip, K.P.; Chitta, R.M. Stabilization of Expansive Soil Using Industrial Wastes. *Geomech. Eng.* **2017**, *12*, 012238.
18. Takeshi, K.; Aly, A.; Toshihide, S. The Use of Recycled Bassanite and Coal Ash to Enhance the Strength of Very Soft Clay in Dry and Wet Environmental Conditions. *Constr. Build. Mater.* **2013**, *38*, 224–235.

19. Wu, Y.K.; Shi, K.J.; Yu, J.L.; Han, T.; Li, D.D. Research on Strength Degradation of Soil Solidified by Steel Slag Powder and Cement in Seawater Erosion. *J. Mater. Civil. Eng.* **2020**, *32*, 04020181. [CrossRef]
20. Asskar, J.C.; Saman, S.K. Microstructure Characteristics of Cement-stabilized Sandy Soil Using Nanosilica. *J. Rock Mech. Geotech.* **2017**, *9*, 981–988.
21. Tongwei, Z.; Xibing, Y.; Yongfeng, D.; Dingwen, Z.; Songyu, L. Mechanical Behaviour and Micro-structure of Cement-stabilised Marine Clay with a Metakaolin Agent. *Constr. Build. Mater.* **2014**, *73*, 51–57.
22. Wang, S.N.; Xue, Q.P.; Zhu, Y.; Li, G.Y.; Wu, Z.J.; Zhao, K. Experimental study on material ratio and strength performance of geopolymer-improved soil. *Constr. Build. Mater.* **2021**, *267*, 120469. [CrossRef]
23. Kai, F.; Jun, Z.Y.; Yang, H.P.; Chao, H.Z. Preparation and Catalytic Performance of Acid-Activated Zinc Slag-Metakaolin Geopolymer. *Bull. Chin. Ceram. Soc.* **2021**, *49*, 2061–2069.
24. Kolovos, K.G.; Asteris, P.G.; Cotsovos, D.M.; Badogiannis, E.; Tsivilis, S. Mechanical Properties of Soilcrete Mixtures Modified with Metakaolin. *Constr. Build. Mater.* **2013**, *47*, 1026–1036. [CrossRef]
25. Wu, Z.L.; Deng, Y.F.; Liu, S.Y.; Liu, Q.W.; Chen, Y.G.; Zha, F.S. Strength and Micro-structure Evolution of Compacted Soils Modified by Admixtures of Cement and Metakaolin. *Appl. Clay Sci.* **2016**, *127–128*, 44–51. [CrossRef]
26. Wang, L.H.; Li, X.Y.; Cheng, Y.; Bai, X.H. Effects of Coal-metakaolin on the Properties of Cemented Sandy Soil and its Mechanisms. *Constr. Build. Mater.* **2018**, *166*, 592–600. [CrossRef]
27. Deng, Y.F.; Wu, Z.L.; Liu, S.Y.; Yue, X.B.; Zhu, L.L. Influence of Geopolymer on Strength of Cement-stabilized Soils and its Mechanism. *Chin. J. Geotech. Eng.* **2016**, *38*, 446–453.
28. Zhang, R.R.; Ma, D.D. Effects of Curing Time on the Mechanical Property and Microstructure Characteristics of Metakaolin-based Geopolymer Cement-stabilized Silty Clay. *Adv. Mater. Sci. Eng.* **2020**, *2020*, 9605941.
29. Ma, D.D.; Ma, Y.Q.; Kun, H.; Zhang, R.R. Pore Structure and Dynamic Mechanical Properties of Geopolymer Cement Soil Based on Nuclear Magnetic Resonance Technique. *Chin. J. Geotech. Eng.* **2021**, *43*, 572–578.
30. Xing, H.F.; Xiong, F.; Zhou, F. Improvement for the Strength of Salt-rich Soft soil Reinforced by Cement. *Mar. Georesour. Geotec.* **2018**, *36*, 38–42.
31. Wu, Z.L.; Zhu, X.Y.; Feng, D.Y.; Liu, H.S. Behavior and Micro-mechanism of Cement-based Modified Compaction Soils Compsed of Steel Slag and Metakaolin. *China J. Highw. Transp.* **2017**, *30*, 18–26.
32. Zhi, T.Y.; Rui, K.; Lian, C.J.; Jun, W. Enhancing Durability of Lime-cement Solidified Sludge with Metakaolin. *Rock Soil Mech.* **2020**, *41*, 1146–1152.
33. Wang, S.N.; Guo, S.F.; Gao, X.Q.; Zhang, P.; Li, G.Y. Effects of Cement Content and Soil Texture on Strength Hydraulic and Microstructural Characteristics of Cement-stabilized Composite Soils. *Bull. Eng. Geol. Environ.* **2022**, *81*, 264. [CrossRef]
34. Anhad, S.G.; Rafat, S. Durability Properties of Self-compacting Concrete Incorporating Metakaolin and Rice Husk Ash. *Constr. Build. Mater.* **2018**, *176*, 323–332.
35. Suksun, H.; Runglawan, R.; Apichat, S.; Avirut, C. Strength Development in Cement Admixed Bangkok Clay: Laboratory and Field Investigations. *Soils Found.* **2011**, *51*, 239–251.
36. Horpibulsuk, S.; Miura, N.; Nagaraj, T. Assessment of Strength Development in Cement-admixed High Water Content Clays with Abrams' law as a basis. *Géotechnique* **2003**, *53*, 439–444. [CrossRef]
37. Miura, N.; Horpibulsuk, S.; Nagaraj, T.S. Engineering Behavior of Cement Stabilized Clay at High Water Content. *Soils Found.* **2001**, *41*, 33–45. [CrossRef]
38. Wang, H.L.; Shen, X.D. Effect of Cement Content on the Early Structual Formation of Stabilized Soil. *Bull. Chin. Ceram. Soc.* **2011**, *30*, 469–473.
39. Cao, Z.G.; Zhang, D.W. Key Parameters Controlling Unconfined Compressive Strength of Soil-cement Mixtures. *Chin. J. Rock Mech. Eng.* **2015**, *34*, 3446–3454.
40. Li, J.J.; Liang, R.W. Research on Compression Strength and Modulus of Deformation of Cemented Soil. *Rock Soil Mech.* **2009**, *30*, 473–477.
41. Suksun, H.; Runglawan, R.; Yuttana, R. Role of fly Ash on Strength and Microstructure Development in Blended Cement Stabilized Silty Clay. *Soils Found.* **2009**, *49*, 85–98.
42. Chu, C.F.; Li, X.C.; Deng, Y.F.; Tang, J.W. Influence of Metakaolin on Mechanical Properties of Cement-modified Marine Soft Soil. *Chin. J. Geotech. Eng.* **2013**, *35*, 170–174.
43. Suksun, H.; Runglawan, R.; Avirut, C.; Yuttana, R.; Apichat, S. Analysis of Strength Development in Cement-stabilized Silty Clay from Microstructural Considerations. *Constr. Build. Mater.* **2010**, *24*, 2011–2021.
44. Azime, S.; Mehmet, E. Effect of Metakaolin Substitution on Physical Mechanical and Hydration Process of White Portland cement. *Constr. Build. Mater.* **2015**, *95*, 257–268.